Spectral Tuning In Quantum Rings By Magnetic Field: Detection From NIR To FIR Regime

Mahdi Solaimani
QUT: Qom University of Technology
Alireza Mobini (ar_mobini2009@yahoo.com)
Islamic Azad University Tehran North Branch https://orcid.org/0000-0002-9836-3381

Research Article

Keywords: semiconducting, magnetic field, absorption spectrum, detection

Posted Date: July 13th, 2021

DOI: https://doi.org/10.21203/rs.3.rs-656071/v1

Version of Record: A version of this preprint was published at Optical and Quantum Electronics on February 5th, 2022. See the published version at https://doi.org/10.1007/s11082-021-03458-x.

Spectral Tuning in Quantum Rings by Magnetic Field: Detection from NIR to FIR Regime

M. Solaimani[1], A. Mobini*[2]
[1]Department of Physics, Qom University of Technology, Qom, Iran.
[2]Department of Electrical and Computer Engineering, Islamic Azad University, Tehran North Branch, Tehran, Iran
Email: ar.mobini@iau-tnb.ir, ar_mobini2009@yahoo.com

ABSTRACT

In this work, we present a quantum ring structure based on semiconducting QWs for spectral tuning in a wide IR range (1.24- 103 μm) using an external magnetic field. We have used a tight binding method to investigate the optical properties of the structure. Using this method the effect of the external magnetic field on the absorption spectrum has been investigated as the post-processing method. Also, the effect of different geometrical parameters like the number of QWs, QR radius, and constructed material considered as processing methods for tuning absorption. The results show for GaAs based QR with the radius of 100/π consist of 4 QWs, absorption peak linearly increase from 100 meV (12.4 um) in LWIR regime and shift to 200 meV (6.2 um) in MIR regime with increasing external magnetic field. Also for a QR with a radius of 200/π, by changing the magnetic field different absorption peaks appear and disappear in an absorption spectrum and a multi-color detector converts to single-detector in the NIR regime. This results help experimentalist to select proper materials with optimized geometrical parameters to achieve desired wavelength for various detection applications.

I. INTRODUCTION

Infrared detectors used in the range of 0.7 um up to hundreds of micrometers have different industrial and technological applications [1-7]. In this filed, movement in this wide range via processing or post-processing method to locate in the desired wavelength is an important issue and attracts much attention [8,9]. A review on spectral selectivity in infrared thermal detection especially those operating at non-cryogenic was made in[8]. In [9] a graphene-based structure used as a tunable mid-infrared biosensor. It showed optical conductivity of graphene affect the resonance frequency that important in detection wavelength. For lower wavelength, Schottky-like contact at the InP nanowire–ITO interface investigated for bias-dependent tuning of the spectral shape of the responsivity of photodetector [10]. In this filed QWs and QDs based detectors play an important role in the progress of tunable IR detectors [10-12] Quantum dot infrared photodetectors (QDIPs) have been used as their bias-voltage-dependent spectral response via the post-processing method [13-15].In [13], bias-dependent spectral in QDIP was used for spectral tunability in the range of 2-12 μm.

In this paper, we have studied the effect of the magnetic field on the absorption spectrum of a ring shape structure consists of quantum wells (QWs) through numerical diagonalization of a one-dimensional tight-binding Hamiltonian. we presented Ring-like structures within the nanometers scale are generally named Quantum Rings (QRs). These structures have been studied both experimentally [16-17] and theoretically. These nano-rings can be fabricated by various techniques[18-24]. Using well known methods like transfer matrix method, K.P method, Hartree-Fock method, Density-functional method, Monte Carlo method and tight binging method and etc. physical properties of the quantum rings can be obtained [24-26]. Some studied have been done to investigate on properties of quantum rings. Among them transport properties in quantum ring under effect of spin orbit interaction [28-29], Fano effect, Aharonov-Bohm effects and persistent currents [30-32] are some of interesting studies. In our earlier works, we have studied the optical properties of clean[33] , two-electron[34], three electrons[35] and impurity included [36] quantum rings and dots through compact density matrix formalism in the effective mass envelop function approach. Then, by using a one-dimensional tight-binding (1D-TB) model we studied the optical properties quantum rings, as a proposal, to be used in THz detection quantum devices [37]. By using a 1D-TB model we have also studied the electronic properties of a quantum ring in the presence of magnetic flux[38]. In the present work, we have studied the effect of vertically applied magnetic field on absorption and used as a post-processing method. Also geometrical parameters like the number of QWs, QR radius, and constructive material studied for tuning absorption response.

II. STRUCTURE AND SIMULATION METHOD

The Schematic of atomic view of a quantum ring with the effective site (quantum well) in the presence of the external applied magnetic field B, depicted in Fig. 1.

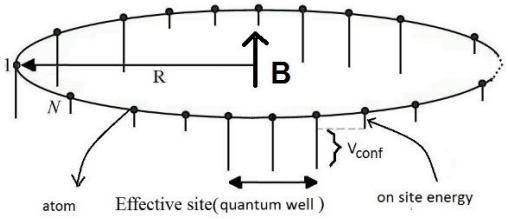

FIG. 1.Schematic of atomic view of a quantum ring with the number of effective site (quantum well) in the presence of the external applied magnetic field B.

The Schematic of atomic view of a quantum ring with the effective site (quantum well) as shown in Fig. 1.

A quantum ring with N numbers of sites of atoms can be modeled by tight-binding Hamiltonian as:

$$\hat{H} = \sum_{n=1}^{N}\left[\left(2t + V_n\right)c_n^{\dagger}c_n - te^{i\theta_{n,n+1}}c_{n+1}^{\dagger}c_n - te^{-i\theta_{n,n+1}}c_n^{\dagger}c_{n+1}\right] \quad (1)$$

Where t, N, $c_n^{\dagger}$ and c_n are the hopping matrix element, the number of sites, and creation and annihilation operators, respectively. Also, the additional on-site potentials V_n form a rectangular potential well of depth V_{Conf} within the circumstance of the quantum ring. $\theta_{n,n+1}$ coms from the magnetic flux ϕ,

$$\theta_{n,n+1} = \frac{e}{\hbar}\int_{r_n}^{r_{+1}} A.dl = \frac{2\pi}{N}\frac{\phi}{\phi_0} \equiv \theta \quad (2)$$

Where, where A is the vector potential, and $\phi_0 = h/e$. By diagonalizing the Hamiltonian from Eq. (1) the eigen energies of the system can be obtained. Now, we study the absorption spectrum which can be calculated from [29]:

$$A\left(E\right) = \frac{1}{N}\sum_{\beta}\delta\left(E - E_{\beta}\right)F_{\beta} \quad (3)$$

where E_{β} is the β energy eigen value, $\delta\ \ E - E_{\beta}$ is the Dirac delta function and F_{β} is the oscillator strength associated with the eigenvalue β, i.e.

$$F_{\beta} = \left[\sum_{n=1}^{N}\psi_n\ \ E_{\beta}\right]^2 \quad (4)$$

Here, $\psi\ \ E_{\beta}$ is the eigenfunction corresponds to energy eigen value E_{β}.

III. SIMULATION AND RESULTS

We consider a quantum ring made of four GaAs/$Al_{0.3}Ga_{0.7}As$ QWs. The barrier has 228 meV height [25]. We assumed the equal widths of the wells and barriers. The ring has a circumstance of 100 nm and m^* is considered as 0.067m0. Using the tight-binding method eigenvalues of the Hamiltonian matrix and corresponding eigen functions for this structure are calculated. Using Eq. (3). absorption spectrum as a function of the photon energy and magnetic flux for GaAs QR consists of 4 QWs and for different values of QR radius: 100/π, 150/π, 200/π, and 250/π calculated and depicted in Fig. 2(a), (b), (c) and (d), respectively. As seen in Fig. 3(a), without a magnetic field, absorption occurs in 100 meV (10.24 um) in the SWIR regime and with applying magnetic field single absorption peak linearly increase and shift to 200 meV (5.1 um) in LWIR regime for B=2. For greater radius, the single peak converts to double and triple peaks in different wavelengths. For R=150/π and 200/π, double peaks occur in 100 and 150 meV and 75 and 100 meV, respectively. For R=250/π, triple peaks occur almost in 50, 75 and 200 meV. These double and triple peaks are fix vs magnetic field.

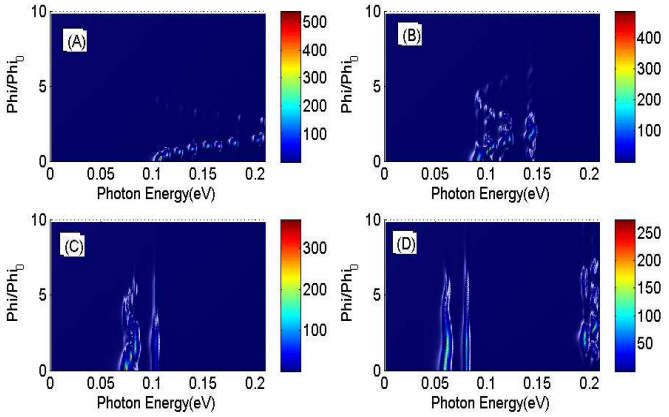

FIG. 2: Absorption spectrum as a function of the photon energy and magnetic flux for GaAs based QR consists of 4 QWs and different values QR radius 100/π, 150/π, 200/π, and 250/π.

In the following, we investigated the effect of the radius in the structure with the lower number of QW. The absorption spectrum as a function of the photon energy and magnetic flux for GaAs based QR consists of 1 QWs and for different values of QR radius i.e. 100/π, 150/π, 200/π, and 250/π calculated and depicted in Fig. 3. For this structure, there is multicolor absorption with definite peaks. For the radius of 100/π, there are two peaks in 31 and 120 meV in LWIR and MIR regimes respectively. When the radius increases to 150/π, three peaks can be seen in absorption in 18, 70 and 145 meV for a low magnetic field. But when the Φ>2.2Φ_0 the first peak in 18 meV disappeared. This occurs for the second peak for Φ>3Φ_0 and only single–color remains in 145 meV. For the radius of 200/π, the peaks are in 12, 42, 92 and 160 meV that covers MIR to the FIR regime. When Φ>2.2Φ_0 the first peak vanished. This occurred for the second peak when Φ>3.2Φ_0. In these conditions, only two peaks remain in 92 and 160 and that by increasing Φ to value of Φ=4.1Φ_0 1 only one peak remains in 160 that makes possible single-color detection. For the greater radius of 250/π, we have a detector with a multi-color absorption spectrum with different peaks from MIR to the FIR regime depicted in Fig. 3(d). A similar trend like the previous (R=250/π) occurred for this detector of greater radius and absorption peaks in lower energies vanish with increasing magnetic field and finally in Φ>5.2Φ_0 the single peak in 174 remains.

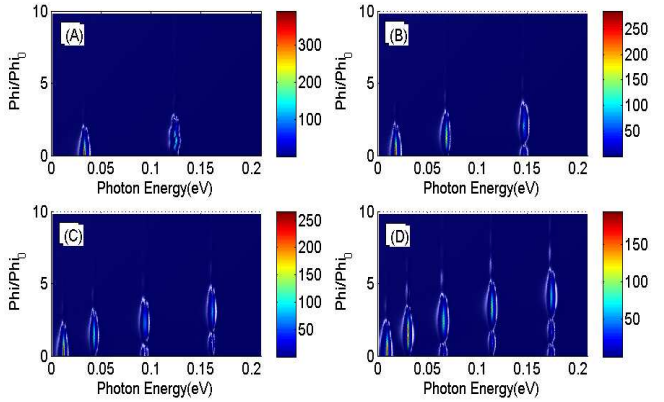

FIG. 3. Absorption spectrum as a function of the photon

energy and magnetic flux for GaAs based QR consists of 1 QWs and different values QR radius 100/π, 150/π, 200/π, and 250/π.

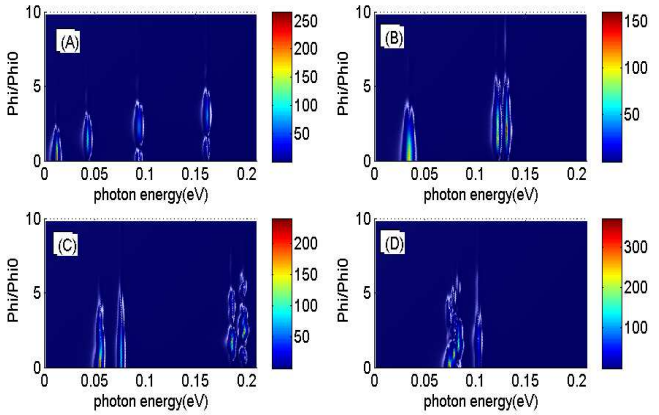

FIG. 4. Absorption spectrum versus photon energy and magnetic flux for GaAs based QR with V_{Conf}= 228 meV, radius = 200/π and different numbers of QW=1, 2, 3 and 4.

In the following, we investigate the effect of the number of QWs on the absorption spectrum. Absorption spectrum versus photon energy and magnetic flux for GaAs based QR with V_{Conf}= 228 meV, radius =(200/π) and different numbers of QW=1, 2, 3 and 4, calculated and depicted in Fig. 4. For the structure based on the one QW, the absorption peak occurs in 12, 42, 92 and 160 meV as discussed before. For a structure based on 2 QWs, four peak integrated to two peaks in 34 and 125 meV with larger FHWM of 13 meV. In this manner the first peak vanished when Φ>4.12Φ_0. Also for 3 number of QWs, double convert to triple peaks in to 54 and 77 and 190 meV and finally for 4 number of QWs, we have double color photodetection in 77 and 103 meV.

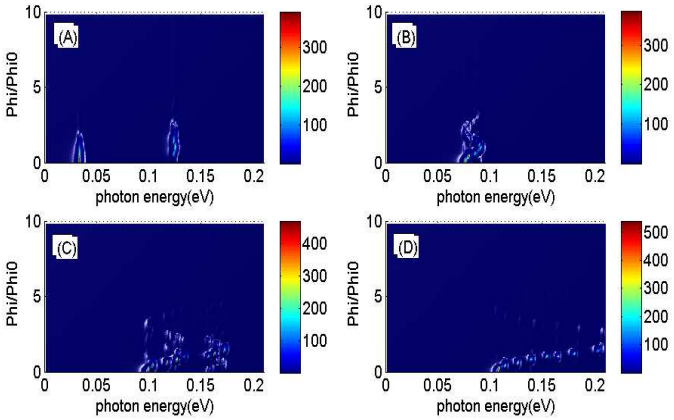

FIG. 5. Absorption spectrum versus photon energy and magnetic flux for GaAs based QR with V_{Conf}= 228 meV, radius =100/π and different numbers of QW=1, 2, 3 and 4.

Now we decrease the radius to 100/π and repeat the calculation. The Absorption spectrum versus photon energy and magnetic flux for GaAs based QR with V_{Conf}= 228 meV, radius =100/π and different numbers of QW=1, 2, 3 and 4 shown in Fig. 5. As seen in Fig. 5(a), for 1 QW based structure, the absorption peaks occur in 31 and 125 meV that the first one's disappears for Φ>2.2Φ_0 and only one peak remains. For 2 QWs based structure double peak integrated to one peak in 80 meV with large FHWM of 14 meV in the lower value of 1.5, but when Φ increased to 2.8Φ_0 the FHWM parameter decreased to 7 meV that leads the sharp absorption. For the structure with 3 number of QWs, there are two wide absorption peaks in 115 and 167 that are fixed vs Φ. But for structure with 4 QW and R of 100/π there is a single color photo response that has blueshift with increasing Φ.

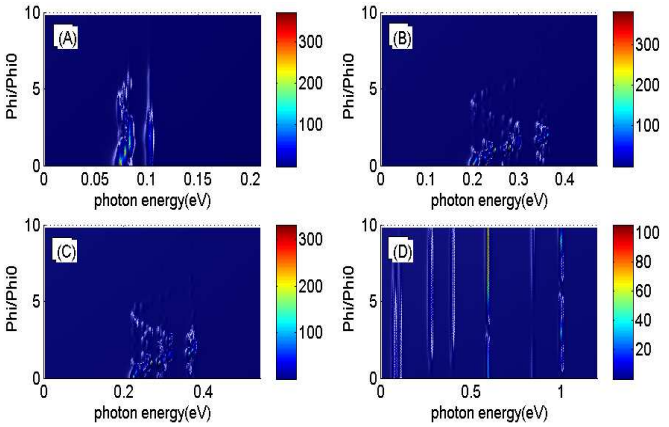

FIG. 6. Absorption spectrum as a function of the magnetic flux and photon energy for QW=4, radius =200/π and different materials GaAs, GaN, InSb, and ZnSe.

Now it's time to investigate the effect of different materials on the absorption spectrum. We have done this for 4 numbers of QW and both 200/π and 100/π radius of QR and different materials of GaAs, GaN, InSb, and ZnSe. The results are shown in Fig. 6 and 7. As seen in Fig. 6(a), (b) and (c), there are wide double peaks in the absorption spectrum that start from 60 meV for GaAs in FIR up to 370 meV for InSb in the MIR regime. But for a ZnSe, there is absorption response with different distinct peaks started from 100 meV up to 1000 meV covering SWIR, MIR, LWIR and NIR regime.

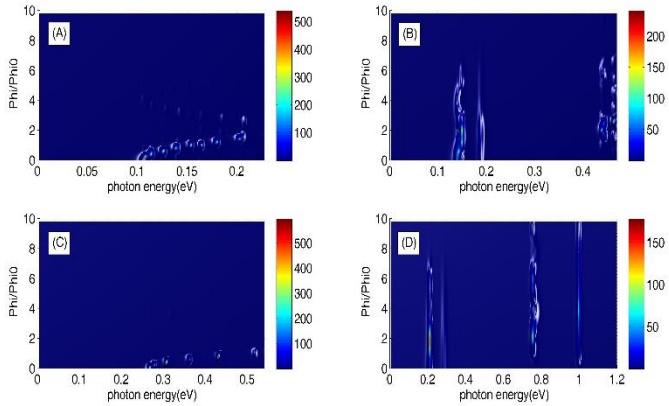

FIG. 7. Absorption spectrum as a function of the magnetic flux and photon energy for QW=4, radius =100/π and different materials GaAs, GaN, InSb, and ZnSe.

Now we decrease the radius to 100/π and repeat the calculation. In this manner, because the size of structure decreased we expect that the number of bands and transitions between them will decrease. The calculated results shown in

Fig. 7. As seen in Fig. 7(a) and (b), there is single-color absorption for GaAs and InSb based structure that linearly increased vs magnetic field. For GaAs based structure absorption starts from 100 meV from LWIR regime for B=0 and increased up 200 meV in MIR regime for B= and the remaining band covered with InSb based structure as started form 250 meV for B=0 and increases up to 500 meV in the SWIR regime. For GaN and ZnSe there are fixed absorption peaks in 140, 190 and 460 and 210, 280, 774and 1000 meV vs magnetic field, respectively. But FWHM of absorption spectrum decreases with an increasing magnetic field.

IV. CONCLUSIONS

In this paper, we examined the absorption spectral tuning of new QR structure with applying the external magnetic field. The wide range of absorption in IR regime achieved for a ZnSe based structure from 100 meV up to 1000 meV covering SWIR, MIR, LWIR and NIR regime. Using the tight-binding method, the effect of other geometrical parameters like QR radius and number of QW investigated on the absorption spectrum and optimized parameters proposed to cover the desired wavelength in the IR range. This comparison helps experimentalist to select proper materials with optimized geometrical parameters to achieve desired optical properties in various optical applications. The results show there wide double peaks in the absorption spectrum that start from 60 meV for GaAs based structure in FIR up to 370 meV for InSb based structure in MIR regime.

REFERENCES

1. Mensz, Piotr M., et al. Journal of Applied Physics **125**, 174505 (2019).
2. Du, X., et al. Journal of Applied Physics **123**, 214504 (2018)
3. Fernandes, F. M., E. C. F. da Silva, and A. A. Quivy, Journal of Applied Physics **118**, 204507, (2015).
4. C.M.S. Negi, D. Kumar, S.K. Gupta, and J. Kumar, IEEE Journal of Quantum Electronics **49**, 839, (2013).
5. S.D. Gunapala, S.V. Bandara, J. K. Liu, J. M. Mumolo, B. Rafol, D. Z. Ting, A. Soibel, and C. Hill, IEEE Journal of Selected Topics in Quantum Electronics **20**, 154, (2014).
6. Rogalski, Antoni, Journal of Applied Physics **93**, 4355 (2015).
7. W. Chen, Z. Deng, D. Guo, Y. Chen, Y. I. Mazur, Y. Maidaniuk, M. Benamara et al. , *Journal of Lightwave Technology* **36**, 2572, (2018).
8. J.Talghader, A. Gawarikar, and R. Shea, *Light Sci Appl* **1,** (2012).
9. Zhu, Yibo, Zhaoyi Li, Yufeng Hao, James Hone, Nanfang Yu, and Qiao Lin. In *2017 19th International Conference on Solid-State Sensors, Actuators and Microsystems (TRANSDUCERS)*, 1340, (2017).
10. Jain, Vishal, Magnus Heurlin, Mohammad Karimi, Laiq Hussain, Mahtab Aghaeipour, Ali Nowzari, Alexander Berg et al. *Nanotechnology* **28**, (2017).
11. Jang, Woo-Yong, Majeed M. Hayat, Payman Zarkesh-Ha, and Sanjay Krishna. *Optics express* **20**, 29823, (2012).
12. Diedenhofen, Silke L., Dominik Kufer, Tania Lasanta, and Gerasimos Konstantatos. *Light: Science & Applications* **4**, (2015).
13.Sakoglu, Unal, Zhipeng Wang, Majeed M. Hayat, J. Scott Tyo, Senthil Annamalai, Philip Dowd, and Sanjay Krishna. In *Nanosensing: Materials and Devices***5593**, 396, (2004).
14. P. Bhattacharya, S. Krishna, J. Phillips, P. J. McCann, and K. Namjou, Journal of Crystal Growth **227**, 27, (2001).
15. S. Krishna, P. Rotella, S. Raghavan, A. Stintz, M. M. Hayat, J. S. Tyo, and S. W. Kennerly, in *Proc. IEEE/LEOS Annual Meeting 2002, New York*, **2**, p. 754, Proceedings of the IEEE, Nov. (2002).
16. N. T. Bagraev, N. G. Galkin, W. Gehlhoff , L. E. Klyachkin and A. M. Malyarenko, J. Phys.: Condens. Matter **20**, 164202, (2008).
17. J. M. Garcia, D. Granados, J. P. Silveira, F. Briones, Microelectronics Journal **35**, (2004).
18. A. Lorke, R. J. Luyken, A. O. Govorov, and J. P. Kotthaus, Phys. Rev. Lett. 84, (2000).
19. R. J. Warburton, C. Schaflein, D. Haft, F. Blickel, A. Lorke, K. Karrai, J. M. Garcia, W. Schoenfeld, and P. M. Petroff, Nature (2000).
20. X. Y. Kong, Y. Ding, R. Yang, and Z. L. Wang, Science**303**, (2004).
21. J. H. He, C. Y. Chen, C. H. Ho, C. W. Wang, M. J. Chen, and L. J. Chen, "Growth and Structural Characterization of SiGe Nanorings,"J. Phys. Chem. **C 114**, 5727, (2010).
22. NW. Strom, Zh. Wang, JH. Lee, Z Y. AbuWaar, Yu.Mazur and GJ. Salamo, Nanoscale Res. Lett. **2**, (2007).
23. X.F. Wang, and P. Vasilopoulos, Physica E **39**, (2007).
24/ A. Emperador, M. Barranco, E. Lipparini, M. Pi, L. Serra, Phys. Rev. B **59**, (1999).
25. P. Vagner , M. Mosko , R. Nemeth , L. Wagner , L. Mitas, Physica E **32**, (2006).
26. B. Jia, Z.Yu, Y.Liu, W. Yao, H. Feng, and H. Ye , Microstruct. **47**, (2010).
27. X.F. Wang, P. Vasilopoulos, Physica E**39**,(2007).
28. S. Jana, N. Bhattacharya, A. Chakrabarti, Physica B**406**, (2011).
29. M. Wang and K. Chang, Phys. Rev. B**77**, 125330, (2008).
30. J. Schelter, P. Recher and B. Trauzettel, Solid State Commun.**152**, 1411, (2012).
31. Y.-C. Zhou, X.-E Yang, H.-Z. Li, Phys. Lett. A **190**, 123, (1990).
32. K. Kobayashi, H. Aikawa, S. Katsumoto, and Y. Iye, Phys.Rev. B **68**, (2003).
33. M. Solaimani, Solid state communications **200**, 66-70, (2014).
34. M. Solaimani, L. Lavaei, and M. Ghalandari., Superlattices and Microstructures **82**, 1, (2015).
35. M. Solaimani, Journal of Computational Electronics **17**, 1135, (2018).
36. M. Ghalandari, and M. Solaimani. Optical and Quantum Electronics **48**, 11, (2016).
37. A .Mobini, and M. Solaimani., Physica E: Low-dimensional Systems and Nanostructures **101**, 162, (2018)/.
38. M. Solaimani, Optical and Quantum Electronics **50**, 7, (2018).